Controlled Ultra-Thin Suboxide Films Generation in Metal-Oxide Systems by Ar⁺Ion Irradiation

Controlled Ultra-Thin Suboxide Films Generation in Metal-Oxide Systems by Ar^+ Ion Irradiation

A V Lubenchenko[1], D S Lukyantsev[1], A B Pavolotsky[2], D A Ivanov[1], O I Lubenchenko[1], I V Ivanova[1], V A Iachuk[1] and O N Pavlov[1]
[1]National Research University "Moscow Power Engineering Institute", Moscow, 111250, Russia
[2]Chalmers University of Technology, Göteborg, 41296, Sweden

Abstract. A method of controlled generation of metal suboxide films is proposed, basing on low-current ion sputtering of native oxides of ultra-thin metallic films and XPS chemical and phase depth profiling. Niobium suboxide ultra-thin films are generated and controlled using this approach.

1. Introduction

Metal-suboxide ultra-thin films are used for manufacture of memristors [1]. Memristors are the base for memory cells and/or bidirectional selectors for resistive random access memory (RRAM) [2]. To generate an oxide layer, various methods are used, i.e. electrostatic spray deposition (ESD) and atomic layer deposition (ALD) [3]. However, controlled production of suboxide layers of a certain thickness is a matter of significant difficulties. In [4], Ar^+ sputtering of a natural metallic oxide layer for generation of a suboxide layer was used and the results of sputtering were observed with the help of X-ray photoelectron spectroscopy (XPS). For interpretation of results, standard methods were used that didn't enable to determine the film thicknesses and oxide phases.

In our research, we used low-current ion sputtering of native oxides on ultra-thin metal films. After each stage of sputtering, depth chemical and phase profile of multi-layer films was controlled by our new method [5]. This approach enabled us to choose sputtering parameters for generation of ultra-thin suboxide films of desired profiles.

2. Experimental Details

In this work, surface oxide structures of a Nb-O system generated by ion modification with Ar. An air-oxidized ultra-thin niobium film was studied by means of XPS. This film 10 nm thick was deposited onto a silicon substrate by magnetron sputtering using the setting Pfeiffer Vacuum SLS630G. The film thickness was controlled during the sputtering process by the known deposition rate.

The photoelectron spectra were recorded by the electron and ion spectroscopy module of the Nanofab 25 (NT-MDT) platform with its hemispherical energy analyzer SPECS Phoibos 225. During the experiment, the residual pressure in the analytical chamber was controlled with a Bayard-Alpert gage and a secondary ion mass spectrometer and it was about 10^{-7} Pa. The X-ray source was SPECS XR 50 with a double Al/Mg anode generating photons with energies of 1486,6 eV and 1253,6 eV correspondingly and located at an angle of to the analyzer axis.

Suboxide structures in the ultra-thin film were generated by Ar^+ ion sputtering. The sputtering procedure was performed with the ion source SPECSIQE 12/38 with an energy of 500 eV at an angle of 70° to the surface normal. The sputtering ion beam was low-current: the ion current was 50 nA, the

duration of each stage of sputtering was 10 minutes, the fluence equaled $3 \cdot 10^{15}$ ions/cm^2. In this operation mode of the ion gun, selective sputtering of oxygen in the film took place (the sputtering rate of oxygen is few times more than that of niobium) and the film itself was depleted of oxygen and suboxide were generated in it. Such delicate sputtering enabled a rather exact approach to the desirable oxide distribution in the film.

3. Depth profiling

One of the most prospecting non-destructive methods for ultra-thin film profiling is XPS with probing depth about 10 nm. The standard XPS method consists in elemental analysis of the film and calculation of relative atomic concentrations based on assumption of the target's depth homogeneity. However, nearly all real subsurface regions are inhomogeneous and multi-component.

For ultra-this films study, we use a non-destructive XPS depth profiling method considering that structures of target surfaces are multilayer, multicomponent and multiphase and enabling to get a chemical and phase depth profile of the surface [5]. This advanced XPS method used by us takes account of multilayer, multicomponent and multiphase structures of target surfaces and enables to obtain surface depth profiles. This method is based on the following features: by background subtraction, difference of surface and bulk energy losses is considered; using of constant parameters for background and line shape calculation in all the range of photoelectron spectra; using of peak shape parameters of the spectra from the Handbook of X-Ray Photoelectron Spectroscopy [6] for pure homogeneous targets; simultaneous interpretation of different peaks of the same element using the same model.

4. Results and Discussion

In this work, surface oxidized structures of Nb-O were studied. For analysis of the Ta-O system, XPS data were taken from [4].

Phase depth profiling was performed by the photoelectron spectra. It enabled to identify chemical compounds in the sample and determine the sequence of layers [7]. For this purpose, an XPS peak was decomposed into partial peaks. The structure of such peaks is complex due to spin-orbit interaction, chemical shift, satellite peaks, etc. The values of binding energies and spin-orbit interaction energies for chemically pure elements were taken from the experimental data of the Handbook of X-ray Photoelectron Spectroscopy [6]. More, peaks may overlap and their shape and width depend on various factors. Peak shapes were described with the Doniach-Sunjich expression and the Voigt function. For peak deconvolution, we used the method described in [8].

Figures 1 and 2 show the deconvolution results of XPS spectra for oxidized systems of Nb 10 nm thick before and after ion sputtering and Ta after two stages of sputtering [4].

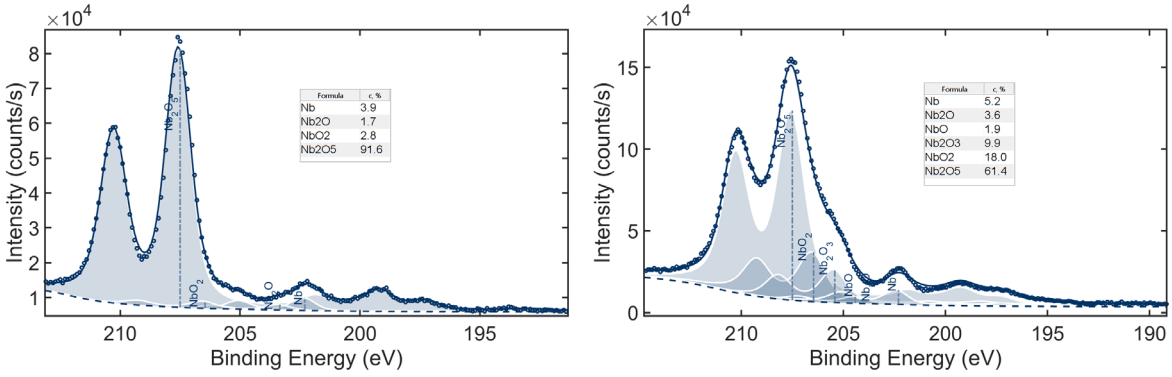

(a) **(b)**

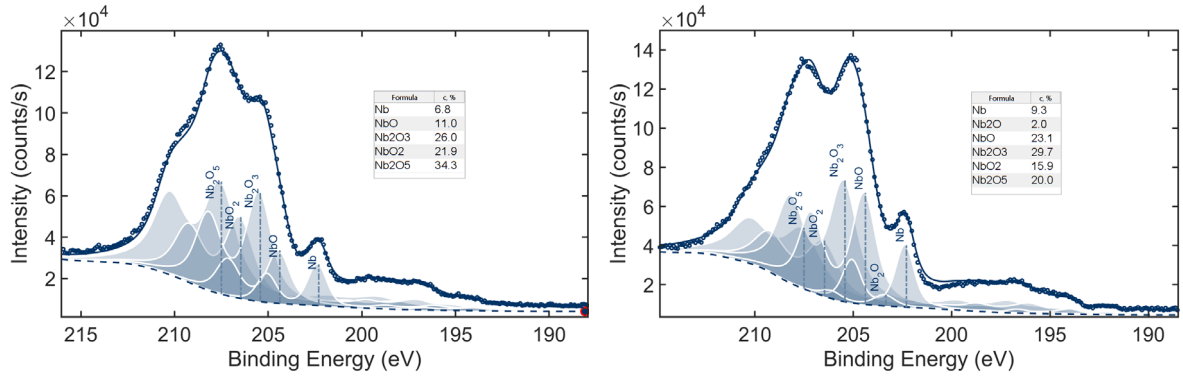

Figure 1 (a, b, c, d). Detailed photoelectron spectra of line Nb 3d of the system NbO_x/Nb/Si: **(a)** prior to modification; **(b)** after the first stage of modification (10 minutes); **(c)** after the second stage of modification (20 minutes); **(d)** after the third stage of modification (30 minutes). Circles: experimental data; solid line: calculation results; filled areas: partial peaks of chemical compounds.

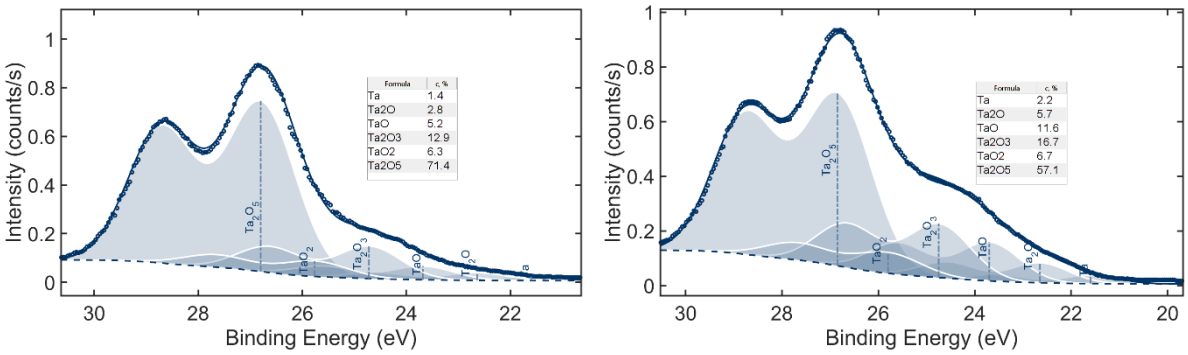

Figure 2 (a, b). Detailed photoelectron spectra of line Ta 3d of the system TaO_x/Ta: **(a)** prior to modification; **(b)** after the first stage of modification (10 minutes); **(c)** after the second stage of modification (20 minutes); **(d)** after the third stage of modification (30 minutes). Circles: experimental data; solid line: calculation results; filled areas: partial peaks of chemical compounds.

As a result of sputtering of the Nb-O system, it was found that the doublet structure of line Nb-3d changed significantly: the Nb_2O_5 peak (the binding energy is approx. 210 eV) softened and disappeared by further sputtering; the peak value of the metallic Nb increased and became more impressive in comparison with the initial value; presence of any chemical compounds was variable. By phase profiling of the Ta-O system before and after sputtering, similar changes of the oxide structure were found.

In Tables 1 and 2, calculation results for surface layer thicknesses of Nb-O and Ta-O systems by ion sputtering are shown. The sequence of suboxide layers in the target prior to ion beam irradiation is determined on the base of the following assumptions. As far as the upper layer contacts with the environment, it is oxidized till the highest rate. Deep into the target, the diffusion constant decreases so each following layer is of smaller oxidation rate than the previous one. A mirror sequence of layers is observed in targets after ion modification. During the first stage of sputtering, the upper oxide layer is subject to the greatest modification. Layers of decreasing oxidation rate in direction to the surface of the sample are generated. This assertion is confirmed by the data of [4]. By further sputtering of targets, layer of various suboxide structures and thicknesses are generated.

Table 1. Chemical and Phase Depth Profiling of a NbO_x/Nb/Si Target

	Before sputtering		After 1st sputtering		After 2st sputtering		After 3st sputtering	
	d (nm)	Formula	*d* (nm)	Formula	*d* (nm)	Formula	*d* (nm)	Formula
6	–	–	0.1	C_xH_y	–	–	–	–
5	1.3	C_xH_y	2.3	0.91 Nb_2O_3 + 0.09 NbO	1.9	NbO	1.1	Nb_2O
4	7.0	Nb_2O_5	3.0	Nb_2O_5	3.3	Nb_2O_3	1.7	NbO
3	0.7	NbO_2	0.7	NbO_2	1.4	Nb_2O_5	2.2	Nb_2O_3
2	1.6	Nb_2O	2.1	Nb_2O	0.4	NbO_2	1.1	0.73 Nb_2O_5 + 0.27 NbO_2
1	–	Nb	–	Nb	–	Nb	–	Nb
Sub.		SiO_2/Si		SiO_2/Si		SiO_2/Si		SiO_2/Si

Table 2. Chemical and Phase Depth Profiling of a TaO_x/Ta Target

	Before sputtering		After 1st sputtering		After 2st sputtering	
	d (nm)	Formula	*d* (nm)	Formula	*d* (nm)	Formula
3	–	–	1.7	TaO	1.9	TaO
4	–	–	3.5	Ta_2O_3	2.6	Ta_2O_3
3	–	–	0.5	TaO_2	0.4	TaO_2
2	8.1	Ta_2O_5	2.8	Ta_2O_5	2.0	Ta_2O_5
1	3.3	Ta_2O	4.1	Ta_2O	4.8	Ta_2O
Sub.	–	Ta	–	Ta	–	Ta

By sputtering of the Nb-O system, it was found that the present hydrocarbon layer prevented full sputtering. During the first stage of sputtering, a larger part of the Nb_2O_5 layer (that was equivalent to 3–3.5 nm thickness) changed its structure. As a result, the subsurface area of the sample was modified, the thicknesses of the initial Nb_2O_5, Nb_2O changed and new Nb_2O_3, NbO layers were generated. The surface structure underwent the greatest changes during the first stage of sputtering.

During the second stage of sputtering, the hydrocarbon layer was totally sputtered that led to more effective sputtering and mixing of other layers due to deeper penetration of argon ions. It was found that a Nb_2O was fully absent: this layer had been dissolved and probably transformed into NbO and Nb_2O_3 layers. It is possible that rapid generation and growth of the Nb_2O_3 layer during two stages of sputtering took place due to its low density compared with other suboxides and its close location to the Nb_2O_5 layer which suffers the greatest change of thickness to its decrease.

During the third stage of sputtering, the thickness of the Nb_2O_5 layer decreased to 0.8 nm. The Nb_2O_3 thickness decreased. It was caused by selective sputtering of oxygen: most part of it moved up participating in generation of the Nb_2O layer thick. As a result of sputtering, small decrease of NbO thickness to 1.7 nm was observed. The thickness of this layer suffered minor changes during the sputtering process by certain constant parameters.

During phase profiling of the Ta-O system, it was found that the Ta_2O layer thickness increased insignificantly from 3.3 nm to 4.8 nm that confirmed penetration of oxygen into deeper layers that is oxygen was “driven”. The TaO_2 layer was generated during the first stage of sputtering and its thickness didn’t really change after the second stage; it probably confirmed that the structure of this compound was stronger and its sputtering rate lesser. The TaO layer thickness changed insignificantly; it confirmed diffusion of oxygen from deeper suboxide layers upwards. The results for oxide and suboxide layer

thicknesses calculated by us coincide have a good agreement with the results reported in [4] with the help of transmission electron microscopy (TEM).

Our investigation shows that the structure of generated suboxide Nb films is always complex, depending on initial film thickness, sputtering conditions. Information about chemical and phase depth profiles of films by certain sputtering parameters will enable to generate films of desired structures for memristors.

References

[1] Strukov D B, Snider G S, Stewart D R and Williams R S 2008 *Nature* **453** 80–3
[2] Yang J J, Pickett M D, Li X, Ohlberg D A A, Stewart D R and Williams R S 2008 *Nature Nanotechnology* **3** 429–33
[3] Salaün A L, Mantoux A, Blanquet E and Djurado E 2009 *J. of The Electrochemical Society* **156** H311
[4] Song W D, Ying J F, He W, Zhuo V Y-Q, Ji R, Xie H Q, Ng S K, Ng S L G and Jiang Y 2015 *Appl. Phys. Letters* **106** 031602
[5] Lubenchenko A V, Ivanov D A, Lubenchenko O I, Yachuk V A, Pavlov O N, Lashkov I A, et al. 2019 *J. of Phys.: Conf. Ser.* **1370** 012048
[6] Moulder J F, Stickle W F, Sobol P E and Bomben K D 1979 *Handbook of X Ray Photoelectron Spectroscopy: A Reference Book of Standard Spectra for Identification and Interpretation of XPS Data* (Physical Electronics)
[7] Lubenchenko A V, Batrakov A A, Ivanov D A, Lubenchenko O I, Lashkov I A, Pavolotsky A B, et al. 2018 *Semiconductors* **5** (52) 678–82
[8] Tanuma S, Powell C J and Penn D R 2003 *Surf. and Interface Analysis* **35** 268–75